Talanta 89 (2012) 264–269

Contents lists available at SciVerse ScienceDirect

Talanta

journal homepage: www.elsevier.com/locate/talanta

# Self-assembled coordination nanoparticles from nucleotides and lanthanide ions with doped-boronic acid-fluorescein for detection of cyanide in the presence of $Cu^{2+}$ in water

Sirinan Kulchat[a], Anusak Chaicham[a], Sanong Ekgasit[a], Gamolwan Tumcharern[b], Thawatchai Tuntulani[a], Boosayarat Tomapatanaget[a,*]

[a] Supramolecular Chemistry Research Unit, Department of Chemistry, Faculty of Science, Chulalongkorn University, 10330 Bangkok, Thailand
[b] National Nanotechnology Center, National Science and Technology Development Agency, Pathumthani 12120, Thailand

ARTICLE INFO

*Article history:*
Received 28 September 2011
Received in revised form 8 December 2011
Accepted 12 December 2011
Available online 17 December 2011

*Keywords:*
Boronic acid
Fluorecein
Self-assembly coordination
Nanoparticle
Cyanide sensing

ABSTRACT

The sensor molecule, **F-*o*BOH**, containing boronic acid-linked hydrazide and fluorescein moieties was synthesized. For anion sensing applications, **F-*o*BOH** was studied in aqueous media. Unfortunately, **F-*o*BOH** was found to be hydrolyzed in water. Therefore, a new strategy was developed to prevent the hydrolysis of **F-*o*BOH** by applying self-assembly coordination nanoparticles network (**F-*o*BOH**-AMP/$Gd^{3+}$ CNPs). Interestingly, the nanaoparticles network displayed the enhancement of fluorescent signal after adding $Cu^{2+}$ following by $CN^-$. The network, therefore, possessed a high selectivity for detection of $CN^-$ compared to other competitive anions in the presence of $Cu^{2+}$. Cyanide ion could promote the $Cu^{2+}$ binding to **F-*o*BOH** incorporated in AMP/$Gd^{3+}$ CNPs to give the opened-ring form of spirolactam resulting in the fourfold of fluorescence enhancement compared to $Cu^{2+}$ complexation without $CN^-$. Additionally, the log K value of **F-oBOH**-AMP/$Gd^{3+}$ CNPs⊂$Cu^{2+}$ toward $CN^-$ was 3.97 and the detection limits obtained from naked-eye and spectrofluorometry detections were 20 μM and 4.03 μM, respectively. The proposed method was demonstrated to detect $CN^-$ in drinking water with high accuracy.



## 1. Introduction

Cyanide ion is severely poisonous to living creatures, cellular respiratory system [1]. Nevertheless, the wide applications of cyanide salts have remained prevalent, such as industrial uses [2,3]. Consequently, unintentionally releasing of cyanide into environment should be extremely aware of. The toxicity and beneficial parts of cyanide anion inspired researchers to develop sensors for detection of cyanide anion. The low concentration cyanide detection in water can be explored by various instrumental methods such as ion selective potentiometry [4], voltammetry [5], indirect atomic absorption spectrometry [6], spectrofluorimetry in flow systems [7,8]. Recently, many researchers have an effort to design various chemosensors for $CN^-$-specific detection. Considerably, the use of this method is beneficial application in terms of inexpensive cost, rapid implementation and providing the low detection limit. For instances, numerous chemosensors in this approach are based on boronic acid derivatives [9–11], Ru(II) containing pyrrolyl quinoxaline [12,13], displacement approach of Cu complex and $CN^-$ [14,15] and amongst other derivatives [16–21].

Nowadays, a number of fluorescein or rhodamine spirolactam derivatives are playing an increasingly important role in the fields of sensing by giving optical changes [22–27]. As widely known in the characteristic of these compounds, the ring-closing form of spirolactam offers nonfluorescent and colorless properties, whereas the ring-opening form enhances a strong fluorescence emission [28–31]. This becomes particularly important when working with a transition metal sensing. The ring-opening form of spirolactam is generated and offers strong fluorescence and color changes. Recently, changing from a spirolactam ring to a ring-opening form can be utilized for the detection of metal ions including $Hg^{2+}$ [32], $Pb^{2+}$ [33], $Fe^{3+}$ [34], and $Cu^{2+}$ [35,36] monitoring the fluorescence enhancement.

Recently, boronic acid moieties have been demonstrated to have high affinities for anions and diol compounds. Yoon and coworkers [37] have developed the fluorescent chemosensors containing boronic acid-linked hydrazide based rhodamine used as $Cu^{2+}$ sensor with respective ring-opening form. Similarly, Franz and coworkers [38] reported the boronic acid-linked hydrazide based fluorescein for detection of $Cu^{2+}$. Since boronic acid-linked hydrazide group was easily hydrolyzed by $Cu^{2+}$ and water. Boronic acid, therefore, was oxidized by $H_2O_2$ before the resultant fluorescein hydrizido 2-imidophenol was utilized to detect copper ion with the fluorescence enhancement in organic solvents. To the best

* Corresponding author. Tel.: +66 2218 7642; fax: +66 2254 1309.
*E-mail address:* tboosayarat@gmail.com (B. Tomapatanaget).

0039-9140/$ – see front matter © 2011 Elsevier B.V. All rights reserved.
doi:10.1016/j.talanta.2011.12.024

of our knowledge, the boronic acid moiety in the mentioned sensors was not used to detect other substrates.

Herein, we have developed the systematic methodology to protect the hydrolysis of boronic acid-linked hydrazide group based fluorescein sensors, **F-*o*BOH**, by applying self-adaptive coordination nanoparticles of nucleotides and lanthanide metal ions. The boronic acid-linked hydrazide based fluorescein sensors, **F-*o*BOH**, was used as turn-on fluorescence sensor for the selective detection of $CN^-$ in the presence of $Cu^{2+}$ in water. Moreover, we have demonstrated that our proposed method can be used to detect $CN^-$ in drinking water with high accuracy.

## 2. Experimental

### 2.1. Instrumentations and materials

Nuclear magnetic resonance (NMR) spectra were recorded on a Varian 400 and Bruker DRX 400 MHz nuclear resonance spectrometers. All of samples were dissolved in deuterated DMSO. The chemical shifts were recorded in part per million (ppm) using a residue proton solvents as internal interference. High resolution mass spectra were determined on Bruker Daltonics DataAnalysis 3.3 with an electrospray ion source using methanol as a solvent. Absorption spectra were measured by a Varian Cary 50 UV–vis spectrophotometer. Fluorescence spectra were performed on a Varian Eclipse spectrofluorometer by personal computer data processing unit. Scanning electron microscopy (SEM) and energy dispersive X-ray (EDS) analysis were performed on a JEOL JSM-6510A with a high resolution of 3.0 nm at 30 kV. Samples were grounded using aluminum stub. Transmission electron microscopy (TEM) was performed on a JEOL JEM 2010 with the field emission gun operated at 200 kV.

### 2.2. Synthesis

#### 2.2.1. Preparation of fluorescein link boronic acid sensor (*F-oBOH*)

Initially, to prepare the spiro form fluorescein hydrazide by treatment of fluorescein with hydrazine hydrate (yield 60%) [38]. In a 100 mL two-necked round bottom flask equipped with a magnetic bar and a reflux condenser, a solution of fluorescein hydrazide (0.173 g, 0.5 mmol) was stirred for 5 min in ethanol (20 mL). Formylphenylboronic acid (0.075 g, 0.5 mmol) in ethanol (30 mL) was added dropwise into the mixture and followed by adding approximately 6 drops of sulfuric acid. The reaction was refluxed overnight under nitrogen atmosphere. Upon completion of the reaction, the solvent was removed under vacuum to obtain a crude product. The crude product was dissolved in ethyl acetate and extracted with water. The organic layer was dried over anhydrous sodium sulfate and evaporated to dryness under reduced pressure to give a white powder which was then recrystallized in hexane/ethyl acetate affording **F-*o*BOH** as a white solid in 85% yield. $^1$H NMR (400 MHz, DMSO-$d_6$): $\delta$ (in ppm) = 9.854 (s, —ArO*H*, 2H), 9.584 (s, —N=C*H*, 1H), 8.170 (s, —BO*H*, 2H), 7.891 ($J$ = 7.2 Hz, d, —Ar*H*, 1H), 7.609 ($J$ = 8.0 Hz, dd, —Ar*H*, 2H), 7.755 (m, —Ar*H*, 1H), 7.492 (m, —Ar*H*, 1H), 7.292 ($J$ = 3.2 Hz, dd, —Ar*H*, 2H), 7.117 ($J$ = 7.2 Hz, d, —Ar*H*, 1H), 6.644 (s, —Ar*H*, 2H), 6.463 (m, —Ar*H*, 4H). $^{13}$C NMR (100 MHz, DMSO-$d_6$): $\delta$ (in ppm) = 163.58, 158.53, 152.41, 150.32, 149.26, 134.47, 133.94, 132.58, 129.08, 128.78, 128.35, 127.88, 126.71, 123.15, 122.31, 111.98, 110.20, 109.96, 102.43, 102.35, 65.37; ESI-HRMS: *m*/*z Anal. Calcd.* for $[M+CH_3OH+H_3O]^+$ = 529.1777, *found* 529.1542. *Anal. Calcd.* for $C_{27}H_{19}BN_2O_6 \cdot 1.25H_2O$: C, 64.76; H, 4.33; N, 5.59. *Found*: C, 64.88; H, 4.04; N, 5.87.

#### 2.2.2. Preparation of *F-oBOH* doped nucleotide/lanthanide CNPs (*F-oBOH*-AMP/$Gd^{3+}$ CNPs)

Coordination nanoparticles were prepared by mixing aqueous mixture of AMP (10 mM, 1.0 mL) and **F-*o*BOH** (0.2 mM, 0.5 mL) and followed by adding the ethanol solution of $Gd(NO_3)_3$ (10 mM, 0.5 mL) into this mixture at room temperature. Finally, the volume of solution was adjusted to be 10 mL by 0.1 M HEPES buffer pH 7.4. Immediately, the colorless precipitate nanoparticles were observed. After stirring the mixture for 1 h, the resultant aqueous suspensions were washed with MilliQ water several times and gathered by ultracentrifugation. Accordingly, the coordination nanoparticles were dispersed in water by sonication. The prepared nanoparticles were examined by SEM, EDS and TEM measurements.

### 2.3. Complexation studies

#### 2.3.1. Complexation studies of *F-oBOH*-AMP/$Gd^{3+}$ CNPs⊂copper(II) with cyanide anion by fluorescence spectrophotometry

All fluorescent experiments were measured in aqueous solution which was prepared by 0.1 M solution of HEPES buffer (pH 7.4) in MilliQ water with sodium chloride as supporting electrolyte. Initially, a 47 μL of $2.15 \times 10^{-3}$ M copper(II) nitrate was added directly to 2.00 mL of $1 \times 10^{-5}$ M **F-*o*BOH**-AMP/$Gd^{3+}$ CNPs in a 1-cm quartz cuvette by micropipette and stirred for a minute. A stock solution of sodium cyanide ($2 \times 10^{-3}$ M) was prepared in HEPES buffer (pH 7.4) and then was added in portion via micropipette (10–80 μL) to a mixture solution of **F-*o*BOH**-AMP/$Gd^{3+}$ CNPs and copper cation. After each addition, the mixture was stirred and the fluorescence spectra were recorded.

#### 2.3.2. Determination of detection limit of *F-oBOH*-AMP/$Gd^{3+}$ CNPs⊂copper(II) with cyanide anion

Typically, 0.1 M solution of HEPES buffer (pH 7.4) was prepared in MilliQ water with sodium chloride as supporting electrolyte. Stock solution of $1 \times 10^{-5}$ M of **F-*o*BOH**-AMP/$Gd^{3+}$ CNPs was prepared in volumetric flask (25 mL). A solution of $2.15 \times 10^{-3}$ M copper(II) nitrate was prepared in MilliQ water in a 10 mL volumetric flask. Fluorescence spectra of **F-*o*BOH**-AMP/$Gd^{3+}$ CNPs with copper (final concentration at $5 \times 10^{-5}$ M) complexes were monitored for 10 times and all data were used to calculate the detection limit. For naked-eyed detection limit, in each portion, the solution of copper cation (47 μL) was added directly to 2.00 mL of $1 \times 10^{-5}$ M **F-*o*BOH**-AMP/$Gd^{3+}$ CNPs in each vial by micropipette and stirred for a minute. The stock solution of cyanide anions ($2 \times 10^{-3}$ M) was added in portion (20–400 μL) to each vial of the mixture solution of **F-*o*BOH**-AMP/$Gd^{3+}$ CNPs and copper cation.

#### 2.3.3. Interference studies by fluorescence spectrophotometry

Typically, 0.1 M HEPES pH 7.4 was prepared in all interference studies. In the cuvette, the solution of $1 \times 10^{-5}$ M **F-*o*BOH**-AMP/$Gd^{3+}$ CNPs (2 mL) and $1 \times 10^{-5}$ M $Cu^{2+}$ and $1 \times 10^{-4}$ M $CN^-$ was added by the miscellaneous anions including $F^-$, $Cl^-$, $Br^-$, $I^-$, $OH^-$, $NO_3^-$, $ClO_4^-$, $BzO^-$, $H_2PO_4^-$ and $SCN^-$ (the amount of foreign anion according to in Table 1). The emission spectra were recorded after stirring for 5 min.

## 3. Results and discussion

### 3.1. Synthesis and characterization of sensory molecules

We have synthesized the sensor, **F-*o*BOH**, by attaching boronic acid and hydrazide linker to fluorescein for detection of cyanide in the presence of $Cu^{2+}$. The synthetic procedure of **F-*o*BOH** is illustrated in Scheme 1. Fluorescein hydrazide was prepared by the addition of hydrazine into the carboxylic moiety of fluorescein

**Table 1**
Effect of interference anions on the determination of $CN^-$ ($C_{CN^-}$ = 24.5 ppm).

| Foreign anion | Equivalent | %Relative error | Interference (M) | Tolerance limit (ppm) |
|---|---|---|---|---|
| $Cl^-$ | 1000 | 0.620 | 0.5000 | 29,220 |
| $Br^-$ | 1000 | 1.248 | 0.5000 | 51,450 |
| $NO_3$ | 1000 | 1.300 | 0.5000 | 42,505 |
| $ClO_4$ | 1000 | 3.610 | 0.5000 | 70,230 |
| $I^-$ | 100 | 7.160 | 0.0500 | 7495 |
| $SCN^-$ | 100 | 8.740 | 0.0500 | 4859 |
| $BzO^-$ | 100 | 4.125 | 0.0500 | 7206 |
| $OH^-$ | 10 | 6.743 | 0.0050 | 200 |
| $F^-$ | 5 | 9.514 | 0.0025 | 145 |
| $H_2PO_4$ | n.d.[a] | n.d.[a] | n.d.[a] | n.d.[a] |

[a] Not determine.

[13]. The desired product was accomplished by coupling fluorescein hydrazide with 2-formylphenylboronic acid in the presence of sulfuric acid (catalyst) followed by refluxing in ethanol under nitrogen atmosphere to afford the imine group linked to the boronic acid unit. **F-*o*BOH** was obtained as a white solid in 85% yield. The $^1$H NMR spectrum of the **F-*o*BOH** showed a singlet signal of imine proton (N=CH) at 9.584 ppm and the boronic acid protons ($B(OH)_2$) at 8.170 ppm. The $^{13}$C NMR spectra of **F-*o*BOH** showed a characteristic peak of spirolactam carbon at 65.447 ppm. In addition, the electrospray high resolution mass spectrum supported the structure of **F-*o*BOH** showing the intense peak at *m*/*z* 529.1542 ($[M+H^+]+CH_3OH+H_2O$).

### 3.1.1. Study on the stability of *F-oBOH* in aqueous solution

According to Franz's report [38], the fluorescein connecting to boronate ester cannot bind any metals strongly due to hydrolysis in aqueous solution. The hydrolysis of **F-*o*BOH** in the presence of $Cu^{2+}$ in aqueous media at pH 7.0 was investigated by using fluorescence spectrophotometry. From Fig. 1a, the fluorescence intensity at 518 nm assigned to the opened-ring form of spirolactam based **F-*o*BOH** was dramatically increased upon the increment of time from 0 to 180 min. The $^1$H NMR spectrum of **F-*o*BOH** in Fig. S2 showed the hydrolysis behavior in a similar fashion to that reported by Ma and coworkers [39]. The hydrazide part of **F-*o*BOH** was cleft to provide fluorescein and formylphenylboronic acid by $Cu^{2+}$ in aqueous. This observation is indicative of the unstable **F-*o*BOH** in the presence of $Cu^{2+}$ in aqueous solution.

### 3.1.2. Use of coordination nanoparticles to solve the problem

To overcome this limitation of the sensor in aqueous solution, we employed a new strategy for a fluorescence turn-on sensor system of **F-*o*BOH** using an adaptive self-assembly of subunits which could spontaneously form by flexibility following the shape of guest molecule in water. Kimizuka and coworkers [40–42] reported

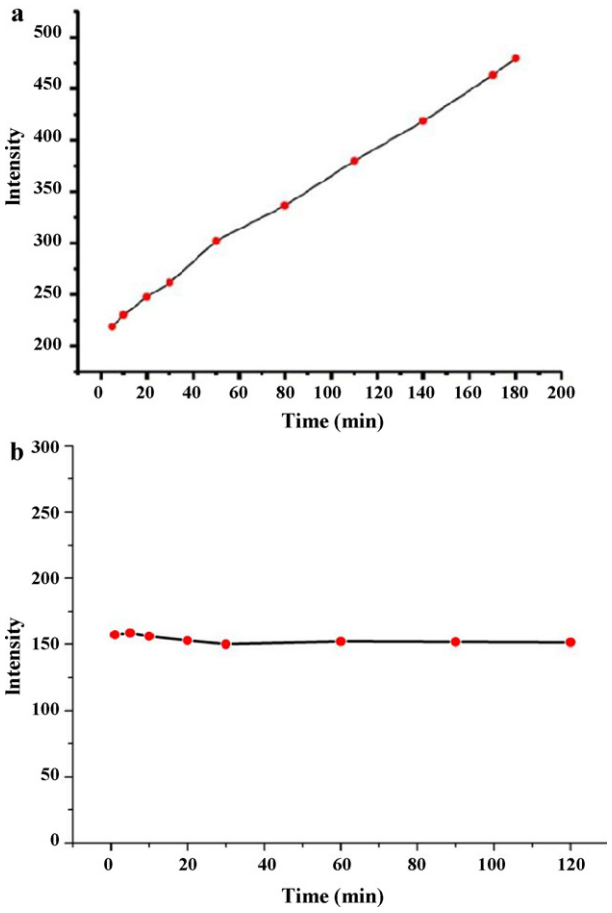


**Fig. 1.** The emission intensity at 518 nm of (a) **F-*o*BOH** and (b) **F-*o*BOH**-AMP/$Gd^{3+}$ CNPs in the presence of copper(II) ion (5 μM) upon various time in the buffered solution pH 7.4 (5% EtOH:water) ($\lambda_{ex}$ = 498 nm).

that the coordination nanoparticles (CNPs) were naturally formed in water by the aids of several nucleotides, lanthanide ions, and dye molecules. In this research, the coordination nanoparticles were prepared by adding gadolinium(III) nitrate ($Gd(NO_3)_3$) into an aqueous mixture of adenosine monophosphate (AMP) and **F-*o*BOH** along with stirring. As shown in Fig. 2, the spherical nanoparticles (**F-*o*BOH**-AMP/$Gd^{3+}$ CNPs) with average diameter of 60 nm were spontaneously formed and characterized by scanning and transmission electron microscopy.

We expected that the coordination nanoparticles would protect the hydrazone unit from hydrolysis due to the interior hydrophobic shell of the coordination nanoparticles. The fluorescence spectra at 515 nm of **F-*o*BOH** incorporated in AMP/$Gd^{3+}$ CNPs in aqueous was

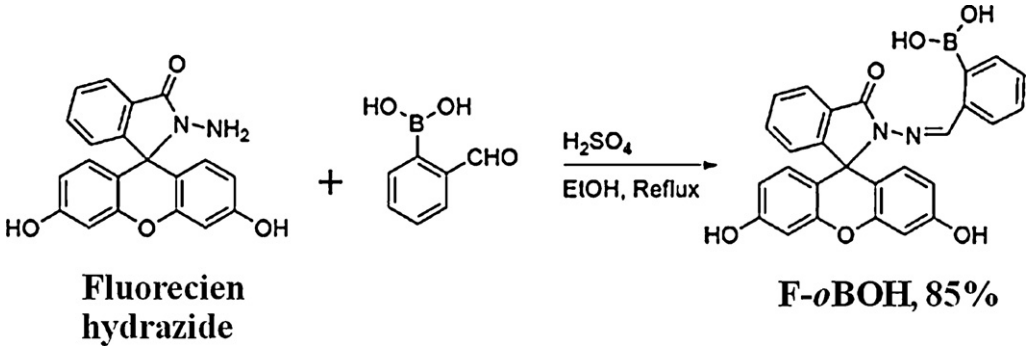


**Scheme 1.** Synthesis pathway of **F-*o*BOH**.

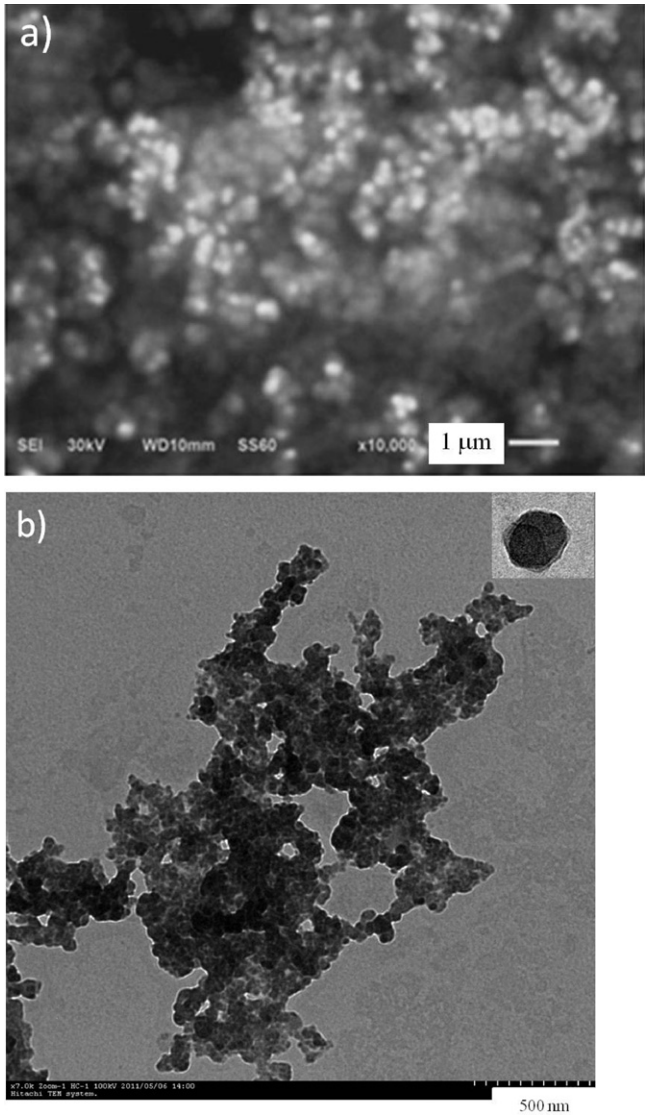


**Fig. 2.** (a) SEM image of **F-*o*BOH**-AMP/$Gd^{3+}$ CNPs and (b) TEM image of **F-*o*BOH**-AMP/$Gd^{3+}$ CNPs.

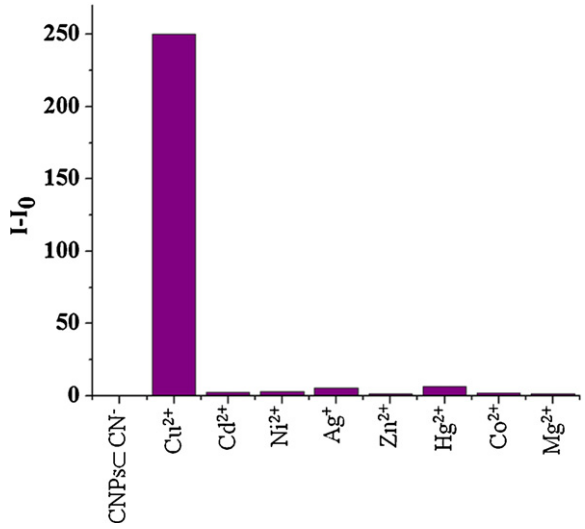


**Fig. 3.** Fluorescence intensity of **F-*o*BOH**-AMP/$Gd^{3+}$ CNPs⊂$CN^-$ at 515 nm in the presence of different cations (50 μM) in HEPES (0.1 M) pH 7.4 ($\lambda_{ex}$ = 492 nm).

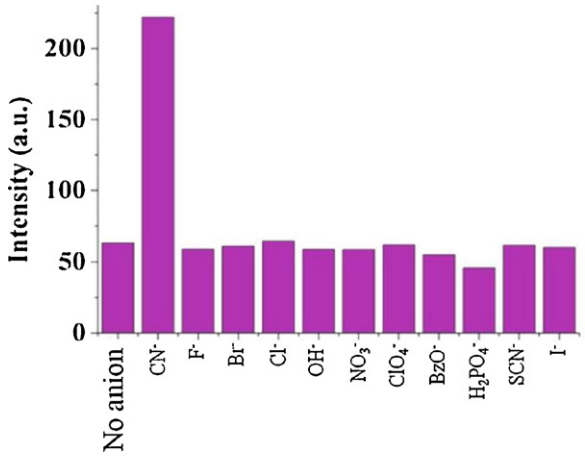


**Fig. 4.** Fluorescence intensity of **F-*o*BOH**-AMP/$Gd^{3+}$ CNPs⊂$Cu^{2+}$ at 515 nm in the presence of different anions (500 μM) in HEPES (0.1 M) pH 7.4 ($\lambda_{ex}$ = 492 nm).

constant upon allowing to stand for 120 min as shown in Fig. 1b. This implied that **F-*o*BOH** incorporated in AMP/$Gd^{3+}$ nanoparticles was very stable in aqueous solution. Therefore, the adaptive coordination nanoparticles network using AMP and $Gd^{3+}$ could protect the hydrolysis of imine based **F-*o*BOH** by water.

### 3.1.3. Study on sensing ability of *F-oBOH-AMP/$Gd^{3+}$ CNPs⊂$CN^-$ toward cations*

In preliminary studies, the fluorescence spectra of **F-*o*BOH**-AMP/$Gd^{3+}$ CNPs⊂$CN^-$ was measured in buffered solution with respective metal cations including $Cu^{2+}$, $Co^{2+}$, $Cd^{2+}$, $Ni^{2+}$, $Ag^+$, $Hg^{2+}$, $Mg^{2+}$ and $Zn^{2+}$. The development of absorption band at 515 nm of the **F-*o*BOH**-AMP/$Gd^{3+}$ CNPs⊂$CN^-$ in the presence of $Cu^{2+}$ is an indicative of the ring-opening form of spirolactam ring based **F-*o*BOH**. In the case of other transition metal ions, from Fig. 3, the fluorescence spectra of **F-*o*BOH** were changed insignificantly. This suggested that **F-*o*BOH**-AMP/$Gd^{3+}$ CNPs showed high selectivity toward $Cu^{2+}$. Therefore, the nanoparticles network in the presence of $Cu^{2+}$ can be used to detect anions using spectrofluorometry.

### 3.1.4. Study on sensing ability of *F-oBOH-AMP/$Gd^{3+}$ CNPs⊂$Cu^{2+}$ toward anions*

Such the boronic acid of **F-*o*BOH** has a vacancy site for anion substitution. Interactions of various anions toward the boron center of **F-*o*BOH**-AMP/$Gd^{3+}$ CNPs were evaluated by spectrofluorometry. As shown in Fig. 4, a fourfold of fluorescence enhancement of **F-*o*BOH**-AMP/$Gd^{3+}$ CNPs⊂$Cu^{2+}$ at 515 nm was particularly observed upon addition of $CN^-$. These results revealed that **F-*o*BOH**-AMP/$Gd^{3+}$ CNPs⊂$Cu^{2+}$ possessed an excellent selectivity toward $CN^-$. Presumably, $CN^-$ bound boronic acid would induce the negative charge on boron center and subsequently promote the coordination of $Cu^{2+}$ on the spirolactam unit resulting in the fluorescent enhancement.

Moreover, the naked-eyed sensing was performed in aqueous as shown in Fig. 5. The color changes from colorless to sky blue and the strong luminescence of **F-*o*BOH**-AMP/$Gd^{3+}$ CNPs⊂$Cu^{2+}$ upon binding with $CN^-$ were remarkably observed. In comparison, **F-*o*BOH**-AMP/$Gd^{3+}$ CNPs⊂$Cu^{2+}$, AMP/$Gd^{3+}$ CNPs in the presence of $Cu^{2+}$ and AMP/$Gd^{3+}$ CNPs in the presence of $Cu^{2+}$ and $CN^-$ did not exhibit any change of optical properties. The results suggested that **F-*o*BOH** in the presence of $Cu^{2+}$ acts as a cyanide sensor in

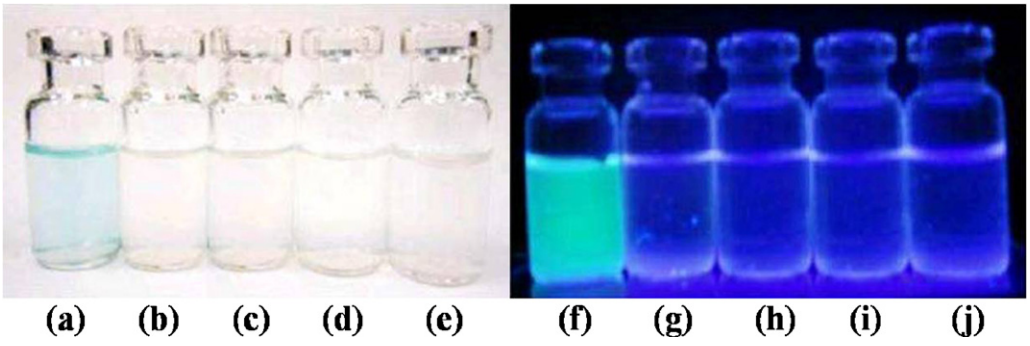


**Fig. 5.** Photograph of Naked-eyes of (a) **F-*o*BOH**-AMP/$Gd^{3+}$ CNPs in the presence of $Cu^{2+}$ 45 equiv. and $CN^-$ 90 equiv., (b) **F-*o*BOH**-AMP/$Gd^{3+}$ CNPs in the presence of $Cu^{2+}$ 45 equiv., (c) AMP/$Gd^{3+}$ CNPs in the presence of $Cu^{2+}$ 45 equiv. and $CN^-$ 90 equiv., (d) AMP/$Gd^{3+}$ CNPs in the presence of $Cu^{2+}$ 45 equiv. and luminescent of (e) **F-*o*BOH**-AMP/$Gd^{3+}$ CNPs in the presence of $CN^-$ 45 equiv. and the samples were illuminated by the 356 nm UV light for (f) **F-*o*BOH**-AMP/$Gd^{3+}$ CNPs in the presence of $Cu^{2+}$ 45 equiv. and $CN^-$ 90 equiv. (g) **F-*o*BOH**-AMP/$Gd^{3+}$ CNPs in the presence of $Cu^{2+}$ 45 equiv. (h) AMP/$Gd^{3+}$ CNPs in the presence of $Cu^{2+}$ 45 equiv. and $CN^-$ 90 equiv. (i) AMP/$Gd^{3+}$ CNPs in the presence of $Cu^{2+}$ 45 equiv. (j) **F-*o*BOH**-AMP/$Gd^{3+}$ CNPs in the presence of $CN^-$ 45 equiv.

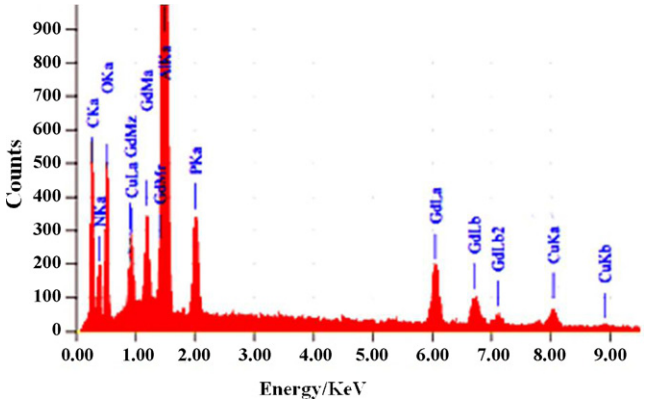


**Fig. 6.** Energy dispersive X-ray spectroscopy (EDS) spectrum of **F*o*BOH**-AMP/$Gd^{3+}$ CNPs⊂$Cu^{2+}$⊂$CN^-$ (Al peak is from the Al stub).

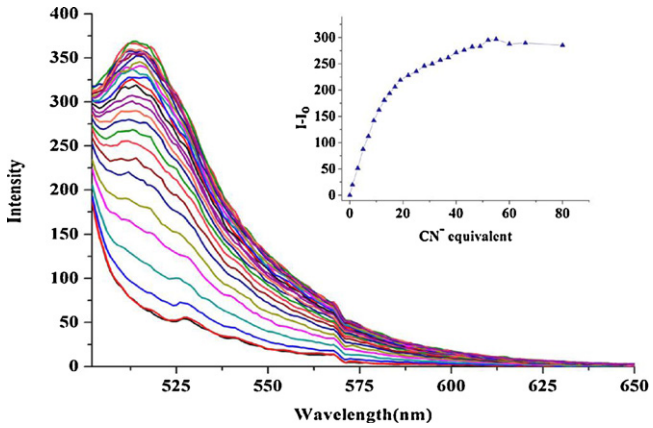


**Fig. 7.** Fluororescence titration spectra of **F-*o*BOH**-AMP/$Gd^{3+}$ CNPs⊂$Cu^{2+}$ in HEPES (0.1 M) pH 7.4 upon addition of $CN^-$ (0–80 equiv.) at emission band at 515 nm. Inset: Titration curve of **F-*o*BOH**-AMP/$Gd^{3+}$ CNPs⊂$Cu^{2+}$ and $CN^-$ ($\lambda_{ex}$, $\lambda_{emis}$ = 492, 515 nm).

aqueous solution giving a visual detection when it was encapsulated in AMP/$Gd^{3+}$ CNPs.

To verify the hypothesis for the structural complexation of **F-*o*BOH**-AMP/$Gd^{3+}$CNPs, The stoichiometry of **F-*o*BOH**-AMP/$Gd^{3+}$CNPs and $Cu^{2+}$ and $CN^-$ was analyzed by Job's plot method. The Job' plot analysis to investigate the stoichiometry of **F-*o*BOH** and $Cu^{2+}$ or $CN^-$ showed the complexation of **F-*o*BOH** incorporated in AMP/$Gd^{3+}$CNPs and $Cu^{2+}$ in a 1:1 binding mode and **F-*o*BOH** incorporated in AMP/$Gd^{3+}$CNPs⊂$Cu^{2+}$ and $CN^-$ also showed the 1:1 stoichiometry (as shown in Figs. S3 and S4).

The results suggested that one $Cu^{2+}$ coordinated to spirolactam and one $CN^-$ bound at a vacancy site of the boron center of **F-*o*BOH**-AMP/$Gd^{3+}$ CNPs⊂$Cu^{2+}$ without the replacement of $CN^-$ on both hydroxyl based boronic acid. Corresponding data from all Job's plot experiments and Kimizuka's reports [43,44], We proposed that $Gd^{3+}$ could bind to the boron center and, thus, possibly function as a linkage on hydroxyl based boronic acid to form **F-*o*BOH**-AMP/$Gd^{3+}$ CNPs.

Additionally, we also characterized the incorporation of $Cu^{2+}$ into **F-*o*BOH**-AMP/$Gd^{3+}$ CNPs using the energy dispersive X-ray spectroscopy (EDS). The **F-*o*BOH**-AMP/$Gd^{3+}$ CNPs⊂$Cu^{2+}$⊂$CN^-$ was prepared and washed with water several times in order to remove the remaining $Cu^{2+}$ and $CN^-$ in the solution. Then, the sample was brought to analyze the incorporated $Cu^{2+}$ and other composition of coordination nanoparticles by EDX analysis.

From Fig. 6, the EDX spectrum shows the characteristic peak of copper element at 8.04 eV (Cu $K_\alpha$), attributing to the incorporated $Cu^{2+}$ in **F-*o*BOH**-AMP/$Gd^{3+}$ CNPs. The characteristic peaks of gadolinium element at 6.05 eV (Gd $K_\alpha$) and phosphorus at 2.01 eV ($PK_\alpha$) assigned to the phosphorous element of adenosine monophosphate (AMP) were also observed. Thus, the EDX analyses give a strong evidence of the formation of $Cu^{2+}$ incorporated into the **F-*o*BOH**-AMP/$Gd^{3+}$ CNPs.

The fluorescence-sensing ability of **F-*o*BOH**-AMP/$Gd^{3+}$ CNPs⊂$Cu^{2+}$ toward $CN^-$ was studied in HEPES pH 7.4. From Fig. 7, the fluorescence emission at 515 nm of the complexation increased as a function of cyanide concentration. The stability constant of **F-*o*BOH**-AMP/$Gd^{3+}$ CNPs⊂$Cu^{2+}$ with $CN^-$ calculated by Specfit 32 program in a 1:1 complexed fashion gives the log *K* values of 3.97 (as shown in Fig. S5).

The detection limit of **F-*o*BOH**-AMP/$Gd^{3+}$ CNPs⊂$Cu^{2+}$ toward $CN^-$ was examined by fluorescence spectroscopy in HEPES pH 7.4 solution providing 4.03 μM (0.198 ppm) which is nearly consistent with the minimum level defined by the World Health Organization [45].

The photograph of **F-*o*BOH**-AMP/$Gd^{3+}$ CNPs⊂$Cu^{2+}$ upon adding the different concentration of the $CN^-$ (20–400 μM) demonstrates the process of color changes of **F-*o*BOH**-AMP/$Gd^{3+}$ CNPs⊂$Cu^{2+}$ from colorless to sky blue. According to Fig. 8, the visual detection limit of **F-*o*BOH**-AMP/$Gd^{3+}$ CNPs⊂$Cu^{2+}$ toward $CN^-$ is approximately 20 μM (0.52 ppm).

### *3.1.5. Effect of interference for determination of $CN^-$ by **F-oBOH**-AMP/$Gd^{3+}$ CNPs⊂$Cu^{2+}$*

The effect of foreign substances was investigated by considering a standard solution of $CN^-$ to the added interference species.

**Fig. 8.** Naked-eyes of **F-*o*BOH**-AMP/$Gd^{3+}$ CNPs⊂$Cu^{2+}$ in HEPES (0.1 M) pH 7.4 in the presence of different concentrations of $CN^-$. From left to right (×10 μM): **F-*o*BOH**-AMP/$Gd^{3+}$, 0, 2.0, 4.0, 7.0, 10.0, 20.0 30.0, and 40.0.

**Table 2**
Determination of $CN^-$ in drinking water sample.

| Added $CN^-$ (μM) | CNP⊂$Cu^{2+}$ | |
|---|---|---|
| | Found (μM) | %Recovery |
| 10 | 10.47 | 105 |
| 15 | 15.67 | 104 |
| 25 | 25.27 | 101 |
| 30 | 30.98 | 103 |
| 45 | 46.29 | 103 |

The tolerance amount and the value (%) of relative error of **F-*o*BOH**-AMP/$Gd^{3+}$ CNPs⊂$Cu^{2+}$ toward anions are collected in Table 1. The evaluated principle for interferences is fixed at a ±10% relative error. From Table 1, it was found that the coexisting substances showed slight effects on the determination of cyanide anion for **F-*o*BOH**-AMP/$Gd^{3+}$ CNPs⊂$Cu^{2+}$. In the case of $H_2PO_4^-$, the tolerance limit value cannot be determined due to the interruption of $H_2PO_4^-$ to the formation of the coordination nanoparticles [41]. Furthermore, $H_2PO_4^-$ caused a pH changes of the solution of **F-*o*BOH**-AMP/$Gd^{3+}$ CNPs⊂$Cu^{2+}$. This implied that **F-*o*BOH**-AMP/$Gd^{3+}$ CNPs⊂$Cu^{2+}$ can be applied to selectively sensing cyanide ion in the coexisting anions.

### *3.1.6. Use of **F-oBOH**-AMP/$Gd^{3+}$ CNPs⊂$Cu^{2+}$ for detecting $CN^-$ in drinking water*

The nanoparticles network in the presence of $Cu^{2+}$ was applied in the analysis of $CN^-$ in commercial drinking water by standard addition as listed in Table 2. Average % recoveries of the spike samples using **F-*o*BOH**-AMP/$Gd^{3+}$ CNPs⊂$Cu^{2+}$ were 103.2. This proposed method, therefore, was a good promising way for $CN^-$ detection.

## 4. Conclusions

We have shown that **F-*o*BOH** could be encapsulated in the adaptive nucleotide/lanthanide coordination nanoparticles, AMP/$Gd^{3+}$ CNPs, to avoid hydrolysis upon using in water. Interestingly, this methodology gave a promising selectivity to detect $CN^-$ in the presence of $Cu^{2+}$ in HEPES pH 7.4 with detection limits obtained from spectrofluorometry and the visual change of 4.03 μM (0.198 ppm) and 20 μM (0.52 ppm), respectively. Furthermore, **F-*o*BOH**-AMP/$Gd^{3+}$ CNPs⊂$Cu^{2+}$ can be used for cyanide sensing without separation of any interference anions even with hydroxide anion. We have demonstrated that this proposed method can be used to detect $CN^-$ in drinking water with high accuracy. Finally, this study would be beneficial in further development of spectroscopic methods for the probe bearing the cleavable active bonds in water.

## Acknowledgements

S.K. is a M.Sc. Student supported by the Junior Science Talent Project (JSTP-06-07) and A.C. is a Ph.D. student under the Royal Golden Jubilee Program (PHD/0235/2552) of the Thailand Research fund (TRF) and Commission on Higher Education (CHE). We also appreciately acknowledge the TRF and CHE (RMU5380003 and RTA5380003) and The National Research University of CHE and the Ratchadaphiseksomphot Endowment Fund (AM1006A) for financial supports. B.T. also thanks the Sensor Research Unit, Department of Chemistry, Faculty of Science, Chulalongkorn University for SEM and EDS analyses.

## Appendix A. Supplementary data

Supplementary data associated with this article can be found, in the online version, at doi:10.1016/j.talanta.2011.12.024.

## References

[1] W. Kaim, B. Schwederski, Bioinorganic Chemistry: Inorganic Elements in the Chemistry of Life, John Wiley & Sons Ltd., England, 1991, p. 208.
[2] X. Lou, L. Qianh, J. Qin, Z. Li, ACS Appl. Mater. Interfaces 1 (2009) 2529–2535.
[3] D. Cho, J.H. Kim, J.L. Sessler, J. Am. Chem. Soc. 130 (2008) 12163–12167.
[4] B. Vallejo-Pecharromán, M.D. Luque de Castro, Analyst 127 (2002) 267–270.
[5] J.M. González LaFuente, E. Fernández Martínez, J.A. Vicente Pérez, S. Fernández Fernández, A.J. Miranda Ordiores, J.E. Sánchez Uría, M.L. Fernández Sánchez, A. Sanz-Medel, Anal. Chim. Acta 410 (2000) 135–142.
[6] A.V. López Gómez, J. Martínez Calatayud, Analyst 123 (1998) 2103–2107.
[7] E. Miralles, D. Prat, R. Compañó, M. Granados, Analyst 122 (1997) 553–558.
[8] D.L. Recalde-Ruiz, E. Andrés-García, M.E. Díaz-García, Analyst 125 (2000) 2100–2105.
[9] C.W. Chiu, Y. Kim, F.P. Gabbaı, J. Am. Chem. Soc. 131 (2009) 60–61.
[10] T.W. Hudnall, F.P. Gabbaı, J. Am. Chem. Soc. 129 (2007) 11978–11986.
[11] M. Jamkratoke, V. Ruangpornvisuti, G. Tumcharern, T. Tuntulani, B. Tomapatanaget, J. Org. Chem. 74 (2009) 3919–3922.
[12] P. Anzenbacher Jr., D.S. Tyson, K. Jursikova, F.N. Castellano, J. Am. Chem. Soc. 124 (2002) 6232–6233.
[13] Y.H. Kimand, J.I. Hong, Chem. Commun. (2002) 512–513.
[14] Q. Zeng, P. Cai, Z. Li, J. Qina, B.Z. Tang, Chem. Commun. (2008) 1094–1096.
[15] V. Ganesh, M.P.C. Sanz, J.C. Mareque-Rivas, Chem. Commun. (2007) 5010–5012.
[16] A. Chaicham, S. Kulchat, G. Tumcharern, T. Tuntulani, B. Tomapatanaget, Tetrahedron 66 (2010) 6217–6223.
[17] J. Isaad, F. Salaün, Sens. Actuators B 157 (2011) 26–33.
[18] J. Ma, P.K. Dasgupta, Anal. Chim. Acta 673 (2010) 117–125.
[19] X. Chen, S.-W. Nam, G.-H. Kim, N. Song, Y. Jeong, I. Shin, S.K. Kim, J. Kim, S. Park, J. Yoon, Chem. Commun. (2010) 8953–8955.
[20] Z. Xu, J. Pan, D.R. Spring, J. Cui, J. Yoon, Tetrahedron 66 (2010) 1678–1683.
[21] Z. Xu, H.-N. Kim, J. Yoon, Chem. Soc. Rev. 39 (2010) 127–137.
[22] M.H. Lee, H.J. Kim, S. Yoon, N. Park, J.S. Kim, Org. Lett. 10 (2008) 213–216.
[23] L. Wu, Y. Dai, G. Marriott, Org. Lett. 13 (2011) 2018–2021.
[24] A. Zumbuehl, D. Jeannerat, S.E. Martin, M. Sohrmann, P. Stano, T. Vigassy, D.D. Clark, S.L. Hussey, M. Peter, B.R. Peterson, E. Pretsch, P. Walde, E.M. Carreira, Angew. Chem. Int. Ed. 43 (2004) 5181–5185.
[25] X.F. Yang, Y. Li, Q. Bai, Anal. Chim. Acta 584 (2007) 95–100.
[26] M.H. Kim, J.H. Noh, S. Kim, S. Ahn, S.K. Chang, Dyes Pigments 82 (2009) 341–346.
[27] T. Li, Z. Yang, Y. Li, Z. Liu, G. Qi, B. Wang, Dyes Pigments 88 (2011) 103–108.
[28] J. Du, J. Fan, X. Peng, P. Sun, J. Wang, H. Li, S. Sun, Org. Lett. 12 (2010) 476–479.
[29] Y.K. Yang, K.J. Yook, J. Tae, J. Am. Chem. Soc. 127 (2005) 16760–16761.
[30] X. Zhang, Y. Shiraishi, T. Hirai, Tetrahedron Lett. 48 (2007) 5455–5459.
[31] M.H. Lee, S.J. Lee, J.H. Jung, H. Lim, J.S. Kim, Tetrahedron 63 (2007) 12087–12092.
[32] H. Yang, Z. Zhou, K. Huang, M. Yu, F. Li, T. Yi, C. Huang, Org. Lett. 9 (2007) 4729–4732.
[33] J.Y. Kwon, Y.J. Jang, Y.J. Lee, K.M. Kim, M.S. Seo, W. Nam, J. Yoon, J. Am. Chem. Soc. 127 (2005) 10107–10111.
[34] Y. Xiang, A. Tong, Org. Lett. 8 (2006) 1549–1552.
[35] Y. Zhou, F. Wang, S.-Y. Kim, J. Kim, J. Yoon, Org. Lett. 11 (2009) 4442–4445.
[36] X. Zhang, Y. Shiraishi, T. Hirai, Org. Lett. 9 (2007) 5039–5042.
[37] K.M.K. Swamy, S.-K. Ko, S.K. Kwon, H.N. Lee, C. Mao, J.-M. Kim, K. Lee, J. Kim, I. Shin, J. Yoon, Chem. Commun. (2008) 5915–5917.
[38] L.M. Hyman, C.J. Stephenson, M.G. Dickens, K.D. Shimizu, K.J. Franz, Dalton Trans. 39 (2010) 568–576.
[39] X. Chen, H. Ma, Anal. Chim. Acta 575 (2006) 217–222.
[40] R. Nishiyabu, C. Aim, R. Gondo, T. Noguchi, N. Kimzuka, Angew. Chem. Int. Ed. 48 (2009) 9465–9468.
[41] C. Aime, R. Nishiyabu, R. Gondo, K. Kaneko, N. Kimizuka, Chem. Commun. (2008) 6534–6536.
[42] C. Aim, R. Nishiyabu, R. Gondo, N. Kimizuka, Chem. Eur. J. 16 (2010) 3604–3607.
[43] R. Nishiyabu, N. Hashimoto, T. Cho, K. Watanabe, T. Yasunaga, A. Endo, K. Kaneko, T. Niidome, M. Murata, C. Adachi, Y. Katayama, M. Hashizume, N. Kimizuka, J. Am. Chem. Soc. 131 (2005) 2151–2158.
[44] R. Nishiyabu, C. Aime, R. Gondo, K. Kaneko, N. Kimizuka, Chem. Commun. 46 (2010) 4333–4335.
[45] Guidelines for Drinking-Water Quality, 3rd ed., World Health Organization, Geneva, 2004, p. 363.